bioRxiv preprint doi: https://doi.org/10.1101/380030; this version posted July 31, 2018. The copyright holder for this preprint (which was not certified by peer review) is the author/funder, who has granted bioRxiv a license to display the preprint in perpetuity. It is made available under aCC-BY-NC-ND 4.0 International license.

Sexually dimorphic gene expression and transcriptome evolution provides mixed evidence for a fast-Z effect in *Heliconius*

Pinharanda A [1], Rousselle M [2], Martin SH [1], Hanly JJ [1], Davey JW [1,3], Kumar S [4], Galtier N [2] & Jiggins CD [1]

[1] Department of Zoology, University of Cambridge, Cambridge, CB2 3EJ, UK

[2] UMR 5554 Institut des Sciences de l'Evolution, CNRS, Université de Montpellier, IRD, EPHE, Place E. Bataillon, Montpellier, France

[3] Department of Biology, University of York, York, YO10 5DD, UK

[4] Institute of Evolutionary Biology, University of Edinburgh, Edinburgh, EH9 3FL, UK

bioRxiv preprint doi: https://doi.org/10.1101/380030; this version posted July 31, 2018. The copyright holder for this preprint (which was not certified by peer review) is the author/funder, who has granted bioRxiv a license to display the preprint in perpetuity. It is made available under aCC-BY-NC-ND 4.0 International license.

Abstract

Sex chromosomes have different evolutionary properties as compared to the autosomes due to their hemizygous nature. In particular, recessive mutations are more readily exposed to selection, which can lead to faster rates of molecular evolution. Here, we report patterns of gene expression and molecular evolution in the sex chromosomes of a group of tropical butterflies. We first improved the completeness of the *Heliconius melpomene* reference annotation, a neotropical butterfly with a ZW sex determination system. Then we sequenced RNA from male and female whole abdomens and female ovary and gut tissue to identify sex and tissue specific gene expression profiles in *H. melpomene*. Using these expression profiles we compare sequence divergence and polymorphism, the strength of positive and negative selection and rates of adaptive evolution for Z and autosomal genes between two species of *Heliconius* butterflies, *H. melpomene* and *H. erato*.

We show that the rate of adaptive substitutions is higher for Z as compared to autosomal genes, but contrary to expectation it is also higher for male as compared to female biased genes. There is therefore mixed evidence that hemizygosity influences the rate of adaptive substitutions. Additionally, we find no significant increase in the rate of adaptive evolution or purifying selection on genes expressed in ovary tissue, a heterogametic specific tissue. Together our results provide limited support for fast-Z evolution. This contributes to a growing body of literature from other ZW systems that also provide mixed evidence for a fast-Z effect.

bioRxiv preprint doi: https://doi.org/10.1101/380030; this version posted July 31, 2018. The copyright holder for this preprint (which was not certified by peer review) is the author/funder, who has granted bioRxiv a license to display the preprint in perpetuity. It is made available under aCC-BY-NC-ND 4.0 International license.

Introduction

Heteromorphic sex chromosomes have different evolutionary properties compared to autosomes (Rice, 1984). Specifically, because recessive mutations are exposed to selection more readily on the sex chromosomes, positive and purifying selection - as well as the strength of genetic drift - are expected to result in different rates of molecular evolution between sex chromosomes and autosomes. An increased evolutionary rate of sex chromosomes relative to autosomes, known as the fast-X effect (Charlesworth *et al.,* 1987), has been observed in *Drosophila* (Ávila *et al.*, 2014). X genes are expected to diverge faster between species than autosomal genes mainly due to the higher substitution rate of recessive, advantageous mutations. However, this process is also influenced by: 1) patterns of selection in males versus females; 2) mutation; 3) recombination and 4) demography (Orr and Betancourt, 2001; Kirkpatrick and Hall, 2004; Vicoso and Charlesworth, 2006; 2009; Pool and Nielsen, 2007; Orr, 2010; Connallon *et al.*, 2012).

Patterns of molecular evolution on the sex chromosomes are particularly influenced by gene expression patterns. Sexually dimorphic expression is often caused by natural and/or sexual selection favouring phenotypes that influence the fitness of one of the sexes (Grath and Parsch, 2016). In species with genetic sex determination the majority of sexually dimorphic traits result from the differential expression of genes present in both male and female genomes (Ellegren and Parsch, 2007). Sex biased expression is common across taxa from mammals (Rinn and Snyder, 2005) to Diptera (Assis *et al.*, 2012), reptiles (Cox *et al.*, 2017), birds (Mank *et al.*, 2010) and Lepidoptera (Rousselle *et al.*, 2016). For example, in *Drosophila melanogaster*, 57% of genes have been categorised as sex biased (Assis *et al.*, 2012); and, in *Heliconius melpomene*, analysis of two different tissues identified up to 29% of expressed genes as sex biased (Walters *et al.*, 2015). The vast majority of genes that exhibit sexually dimorphic expression are active in reproductive tissues and tend to also have distinctive rates of molecular evolution compared to genes without dimorphic expression

bioRxiv preprint doi: https://doi.org/10.1101/380030; this version posted July 31, 2018. The copyright holder for this preprint (which was not certified by peer review) is the author/funder, who has granted bioRxiv a license to display the preprint in perpetuity. It is made available under aCC-BY-NC-ND 4.0 International license.

(Parisi *et al.*, 2003; 2004; Avila *et al.*, 2015). Ultimately, the identification of sex biased genes and subsequent analysis of patterns of molecular evolution will contribute to a better understanding of the evolutionary forces shaping sex chromosome and autosome evolution (Kirkpatrick and Hall, 2004; Zhang *et al.*, 2004; Assis *et al.*, 2012).

Empirical studies of the fast-X effect typically measure two different metrics: 1) the ratio of non-synonymous to synonymous substitution rates (dN/dS); and 2) the amount of adaptive evolution (α) using the McDonald-Kreitman (MK) test (McDonald and Kreitman, 1991). Studies measuring dN/dS usually test for "faster-X divergence". Although this approach may be useful for comparing sex chromosome and autosomal divergence measuring only the relative rate of non-synonymous substitutions captures the effects of both adaptive and neutral (or slightly deleterious) mutations. Estimates of α can better test for an excess of adaptive substitution in the sex chromosome ("faster-X adaptation") by combining measures of within-species polymorphism and between-species divergence, but α is still sensitive to the rate of accumulation of slightly deleterious mutations and demography (Fay 2011). For instance, an increase in N_e is expected to result in decreased dN/dS and increased α even when the rate of adaptive substitutions remains unchanged. To overcome this problem extensions of the MK test such as ω_a were developed to estimate the rate of adaptation by calculating the frequency distribution of polymorphism after correcting for demographic history and distribution of deleterious effects at functional sites (Galtier, 2016).

The analysis of evolutionary rates between sex and autosomal genes, however, has produced mixed evidence in support of fast-X evolution (Meisel and Connallon, 2013). In some taxa there is strong evidence for faster-X divergence but not faster-X adaptation or vice versa (Meisel and Connallon, 2013). For example, the first calculations of faster-X divergence were carried out in *Drosophila* where support for elevated dN/dS in X genes has been mixed. Studies that used autosome-to-X translocations to control for gene content effect did not reach a consensus on the existence of faster-X divergence (Counterman

bioRxiv preprint doi: https://doi.org/10.1101/380030; this version posted July 31, 2018. The copyright holder for this preprint (which was not certified by peer review) is the author/funder, who has granted bioRxiv a license to display the preprint in perpetuity. It is made available under aCC-BY-NC-ND 4.0 International license.

et al. 2004; Thornton *et al.*, 2006; Zhou and Bachtrog, 2012) but X-linked duplicate genes have elevated dN/dS compared to autosomal duplicates (Thornton and Long, 2002). Signals of faster-X sequence divergence in *Drosophila* have been shown to affect non-coding regulatory regions as well, and might be at least partly explained by differences in gene composition on the X versus the autosomes (Hu *et al.*, 2013). However, faster-X divergence in other taxa has received stronger support. For example in humans, chimpanzees and rodents dN/dS is higher for X genes (Nielsen *et al.*, 2005; Mank,Vicoso, *et al.*, 2010).

In contrast, whole-genome analyses of adaptive substitutions have resulted in stronger evidence for faster-X adaptation in *Drosophila* (Mackay *et al.*, 2012), while support for faster-X adaptation in vertebrates is less clear. McDonald-Kreitman tests support faster-X adaptation in wild mouse populations (Baines and Harr, 2007) but, for the European rabbit (*Oryctolagus cuniculus*), a clear faster-X adaptation signal is only present in populations with large effective population sizes (Carneiro *et al.*, 2012).

Taxa with ZW sex determination provide an interesting contrast. For female-heterogametic taxa such as birds, females only have one copy of the Z chromosome. A fast-Z effect may be expected to result from the expression of recessive mutations on the Z chromosome as Z genes are immediately exposed to selection in females (Charlesworth *et al.,* 1987). In birds, fast-Z divergence has been reported, but Z male biased genes were not less accelerated than unbiased genes or female biased genes (Wright *et al.*, 2015). This would not be expected if the fast-Z effect was driven by recessive beneficial mutations, and so it was suggested that fast-Z in birds does not reflect positive selection (Mank, Nam, *et al.*, 2010; Wright *et al.*, 2015).

For Lepidoptera results have also been mixed. Sackton *et al.* (2014) reported that faster-Z evolution was driven by position selection in silkworms. But, in satyrine butterflies, there were no significant differences in adaptive evolutionary rates

bioRxiv preprint doi: https://doi.org/10.1101/380030; this version posted July 31, 2018. The copyright holder for this preprint (which was not certified by peer review) is the author/funder, who has granted bioRxiv a license to display the preprint in perpetuity. It is made available under aCC-BY-NC-ND 4.0 International license.

between the Z and the autosomes (no fast-Z adaptation). However, the comparison of male biased, female biased and unbiased Z genes in satyrine butterflies revealed increased purifying selection against recessive deleterious mutations in female biased Z genes (Rousselle *et al.*, 2016). Considerable uncertainty therefore remains regarding the prevalence and magnitude of the fast-X/Z effect on divergence and adaptation.

Here we investigate the effects of hemizygosity on the rates of adaptive substitution in the neotropical butterfly genus *Heliconius,* a ZW sex determination system, by analysing polymorphism, divergence and gene expression genome-wide. We test whether there is a fast-Z effect in *Heliconius* using two species from the *H. melpomene* and *H. erato* clades which diverged 13 million years ago (synonymous divergence = 0.16) (Kozak *et al.,* 2015; Martin *et al.,* 2016). Previous analyses of *Heliconius* transcriptome data have focused on the evolution of dosage compensation and the impact of sex specific dosage on the levels of gene expression (Walters *et al.*, 2015). In this study, using the same transcriptome data, we first compute sex biased expression. Then, accounting for sex biased gene expression, we: 1) calculate coding sequence divergence and polymorphism in *H. melpomene*; and 2) assess the strength of positive and negative selection, and rates of adaptive evolution between *H. melpomene* and *H. erato*. We then analyse newly generated female transcriptome data from *H. melpomene* ovary and gut tissue in order to investigate whether genes expressed in the reproductive tissue of the heterogametic sex have higher rates of adaptive evolution than those expressed in somatic tissues.

Material and Methods

Updated *H. melpomene* annotation

bioRxiv preprint doi: https://doi.org/10.1101/380030; this version posted July 31, 2018. The copyright holder for this preprint (which was not certified by peer review) is the author/funder, who has granted bioRxiv a license to display the preprint in perpetuity. It is made available under aCC-BY-NC-ND 4.0 International license.

The Hmel2 annotation of the *H. melpomene* genome has 13 178 predicted transcripts spanning 16 897 139 bp (The Heliconius Genome Consortium, 2012; Davey et al., 2016). The Hmel2 annotation is incomplete, as there are 20 118 high quality predicted transcripts in *H. erato* spanning 33 669 374 bp (van Belleghem et al., 2017). To improve the completeness of the annotation for *H. melpomene* we downloaded RNA-seq reads from NCBI repositories ArrayExpress ID: E-TAB-1500 (Briscoe et al., 2013), and BioProject PRJNA283415 (Walters et al., 2015), published since Hmel1 release. We also used data from 10 wing RNA-seq libraries (Hanly 2017). We used the BRAKER1 pipeline to perform unsupervised RNA-seq based genome annotation (Hoff *et al.*, 2016). GeneMark-ET was used to perform iterative training, generating initial gene structures and AUGUSTUS was used for training and subsequent integration of RNA-seq read information into the final gene predictions (Stanke et al., 2008; Lomsadze et al., 2014; Hoff et al., 2016). This resulted in 26,017 predicted transcripts spanning 32,222,367 bp. 6,532 of these transcripts were considered repeat proteins based on 90% single hit match to repeat databases Repbase were removed (Bao *et al*., 2015). We transferred 428 manually annotated genes (441 transcripts/protein) from the original Hmel2 annotation and removed any BRAKER1 predictions that overlapped. We also transferred 189 genes (189 transcripts/proteins) that have been manually annotated and published since Hmel2 release. Specifically, we transferred 73 gustatory receptors; 31 immune response and 85 Glutathione-S-transferases and Glucuronosyltransferases (Briscoe et al., 2013; van Schooten et al., 2016; Yu et al., 2016) and removed any BRAKER1 predictions that were overlapping. Moreover, BRAKER1 predictions that had 1-to-1 overlaps with Hmel2 names were replaced by their original Hmel2 name. For many-to-1 mapping between the BRAKER1 predictions and Hmel2, Hmel2 names were reused and a suffix of g1/g2/g3/etc was added. The rest were renamed from HMEL030000 onwards.

Samples for gene expression analysis

bioRxiv preprint doi: https://doi.org/10.1101/380030; this version posted July 31, 2018. The copyright holder for this preprint (which was not certified by peer review) is the author/funder, who has granted bioRxiv a license to display the preprint in perpetuity. It is made available under aCC-BY-NC-ND 4.0 International license.

Gene expression data was calculated using: 1) Illumina 100bp paired-end RNA-seq data from 5 Panamanian *H. m. rosina* whole-male abdomens, and 5 Panamanian *H. m. rosina* whole-female abdomens, downloaded from GenBank (BioProject PRJNA283415) (Walters *et al.*, 2015); and 2) newly sequenced Illumina HiSeq 2500 150bp paired-end directional (stranded) RNA-seq data from ovary tissue of 7 young (1h) and 6 old (20 days) *H. m. rosina* females, and from gut tissue of 6 young (1h) and 6 old (20 days) *H. m. rosina* females (25 samples from 13 different individuals, Supplementary Table S1).

For these 25 samples *H. m. rosina* females were reared in insectaries in Gamboa, Panama. *Passiflora platyloba* potted plants were monitored daily and 5th instar caterpillars were removed and taken to the laboratory in large individual containers where they were allowed to pupate and emerge at a constant temperature (24-25ºC). The pupating containers in the laboratory were monitored several times a day. When a female emerged, it was either: 1) returned to the insectaries to be mated to a *H. m. rosina* male (Treatment: old, Supplementary Table S1); or 2) dissected 1h after eclosion under controlled laboratory conditions (Treatment: young, Supplementary Table S1). Mated females were kept in individual 1m x 1m x 2m cages for 20 days until dissection.

Guts and ovaries were dissected in RNAlater (ThermoFisher, Waltham, MA) at 24-25ºC and tissue was stored in RNAlater at 4ºC for 24h and -20ºC thereafter. Total RNA was extracted with a combined guanidium thiocyanate-phenol-chloroform and silica matrix protocol using TRIzol (Invitrogen, Carlsbad, CA), RNeasy columns (Qiagen, Valencia, CA) and DNaseI (Ambion, Naugatuck, CT). mRNA was isolated from total RNA via poly-A pull-down, and directional cDNA library preparation and sequencing (Illumina HiSeq 2500, 150bp paired end) were performed by Novogene Bioinfomatics Technologies (Hong Kong, China) (Supplementary Table S1).

bioRxiv preprint doi: https://doi.org/10.1101/380030; this version posted July 31, 2018. The copyright holder for this preprint (which was not certified by peer review) is the author/funder, who has granted bioRxiv a license to display the preprint in perpetuity. It is made available under aCC-BY-NC-ND 4.0 International license.

Read mapping, counting and identification of sex and ovary and gut biased genes

FASTQ reads were aligned to gene sequences from *H. melpomene* v2.5 annotation using HISAT2 (Kim *et al.*, 2015) with default mapping parameters. Mapping statistics were calculated using samtools flagstat (v1.2) (Li *et al.*, 2009). We used htseq-count to determine the number of aligned sequencing reads mapped to each genic feature (HTSeq v0.6.1; python v2.7.10; option: -m union) (Anders *et al.*, 2015).

Estimation of variance-mean dependence from the count data was performed with DESeq2 (v1.14.1) (Love *et al.*, 2014) using Bioconductor v3.4 and R v3.2.5, using the constructor function DESeqDataSetFromHTSeqCount(design=~batch+sex) for sex biased genes and DESeqDataSetFromHTSeqCount(design=~batch+tissue) for ovary and gut biased genes. All the result tables were built using the DESeq2 results() function (options: betaPrior=false, test=Wald). We filtered the results as in Walters *et al.* (2015) with FDR < 0.05 (alpha=0.05) (Walters *et al.*, 2015). We defined male, female and unbiased genes as in Rousselle *et al.* (2016); male biased genes have $\log_2$ fold change significance threshold < 0.66 (option: lcfThreshold<0.66), female biased genes have $\log_2$ fold change significance threshold > 1.5 (option: lcfThreshold>1.5) and the others were classified as unbiased.

Extraction of orthologous genes, coding sequence alignment and SNP calling

OrthoFinder was used to identify orthologous groups of genes in the *H. melpomene* and the *H. erato* transcriptomes (options: -t 48 -a 6). 1-1 orthologous gene sequences were selected for use in subsequent analysis (Supplementary Table S2). Using Gff-Ex, a genome feature extraction package (Rastogi and Gupta, 2014), we extracted coding sequences from: 1) 10 whole-genome short-

bioRxiv preprint doi: https://doi.org/10.1101/380030; this version posted July 31, 2018. The copyright holder for this preprint (which was not certified by peer review) is the author/funder, who has granted bioRxiv a license to display the preprint in perpetuity. It is made available under aCC-BY-NC-ND 4.0 International license.

read re-sequenced wild *H. m. rosina* from Panama (Supplementary Table S3; Van Belleghem et al., 2018) mapped to Hmel2 (Davey *et al.*, 2016) with bwa-mem (Li and Durbin, 2009); 2) the reference *H. erato* genome (Van Belleghem *et al.*, 2017).

For the 10 whole-genome re-sequence *H. m. rosina* samples (van Belleghem *et al.*, 2018), genotypes were called using HaplotypeCaller (GATK v3.4-0-g7e26428) (DePristo *et al.*, 2011), and genotypes were designated as missing if the read depth for a given individual at a given site was <8. Coding sequences for 1-1 orthologous genes were extracted in fasta format from 1) and 2) and aligned using MACSE, accounting for frameshifts and stop codons (Ranwez *et al.*, 2011).

Calculation of diversity and selection statistics for 1-1 ortholog alignments between *H. melpomene* and *H. erato*: *Classic approach*.

The adaptive substitution rate was estimated by comparing synonymous and non-synonymous variation in the polymorphism and divergence compartments, as first proposed by McDonald & Kreitman, 1991; see also Bustamante *et al*., 2005, and Mcpherson *et al*., 2007). We first used the original MK test (referred to as *Classic approach* hereafter) to estimate the rate of adaptive substitution for all genes found to be orthologous between *H. melpomene* and *H. erato.* We calculated: 1) synonymous polymorphism (P_s) and 2) non-synonymous polymorphism (P_n) in *H. melpomene,* as well as 3) synonymous fixed divergence (dS), and 4) non-synonymous fixed divergence (dN) between *H. melpomene* and *H. erato*. We estimated the rate of adaptive molecular evolution (α) between the two species as:

$$\alpha = 1 - \frac{dS\ x\ P_n}{dN\ x\ P_s}$$

bioRxiv preprint doi: https://doi.org/10.1101/380030; this version posted July 31, 2018. The copyright holder for this preprint (which was not certified by peer review) is the author/funder, who has granted bioRxiv a license to display the preprint in perpetuity. It is made available under aCC-BY-NC-ND 4.0 International license.

α assumes that non-synonymous mutations are either adaptive, neutral, or strongly deleterious (McDonald and Kreitman, 1991), with $-\infty > \alpha \geq 1$, where $\alpha = 0$ represents the null hypothesis that non-synonymous mutations are neutral ($dN/dS = P_n/P_S$). $\alpha > 0$ corresponds to $dN/dS > P_n/P_S$ and indicates positive selection, whereas $\alpha < 0$ cprresponds to $dN/dS < P_n/P_S$ and indicates negative selection. These values were calculated using the EggLib C++ function polymorphismBPP (v2.1.11) (De Mita and Siol, 2012) and Bio++ (v2.2.0) (Dutheil and Boussau, 2008) in python (v2.7.5) using scripts adapted from https://github.com/tatumdmortimer (last accessed 09/04/2018) (O'Neill *et al.*, 2015).

Calculation of diversity and selection statistics for 1-1 ortholog alignments between *H. melpomene* and *H. erato*: *Modelling approach*.

The *Classic approach* to the MK test is robust to differences in mutation rates and variation in coalescent histories across genomic locations (McDonald & Kreitman, 1991). Inference of positive selection using the *Classic approach* of the MK test is not robust, however, to the occurrence of slightly deleterious mutations and demographic change. To account for these confounders, we used a *Modelling* approach to estimate the strength of positive and purifying selection in addition to the *Classic approach* described above, using the method of Eyre-Walker and Keightley (2009) as implemented in Galtier (2016) and Rousselle *et al.* (2016).

The *Modelling approach* uses the frequency distribution of polymorphism to assess the distribution of deleterious mutations at functional sites. This elaborates on the *Classic approach* of the MK test by modelling the distribution of fitness effects (DFE) of deleterious non-synonymous mutations as a negative Gamma distribution. The model is fitted to the synonymous and non-synonymous site frequency spectra (SFS) and the expected dN/dS under near-neutrality is

bioRxiv preprint doi: https://doi.org/10.1101/380030; this version posted July 31, 2018. The copyright holder for this preprint (which was not certified by peer review) is the author/funder, who has granted bioRxiv a license to display the preprint in perpetuity. It is made available under aCC-BY-NC-ND 4.0 International license.

304 inferred. The difference between the observed and expected dN/dS provides an
305 estimate of the proportion of adaptive non-synonymous substitutions (α). The per
306 mutation rate of adaptive substitutions is calculated as:

$$\omega_a = \alpha \, x \, \frac{dN}{dS}$$

307 and the per mutation rate of non-adaptive substitutions is calculated as:

$$\omega_{na} = (1 - \alpha) \, x \, \frac{dN}{dS}$$

308

309 **Gene expression level and π_n/π_s ratios**

310 We calculated reads per kilobase per million (RPKM) as:

$$RPKM = \frac{N_c x 10^9}{N_{tot} x L_c}$$

311 To test whether gene expression level and chromosome type have a significant
312 effect on π_n/π_s ratios we used a multiple regression analysis. We established the
313 linear model:

$$\log(\pi_{nij}) \sim \log(\pi_{nsj}) + chromosome\_type_j + \log(RPKM)$$

314 using R (v3.2.5). Where N_c is the number of reads mapped to the genic feature,
315 N_{tot} is the total number of reads mapped in the sample, and L_c is the length of the
316 genic sequence in base pairs (Mortavazi *et al.*, 2008). $RPKM_i$ is the mean RPKM
317 of gene *i* across the 10 individuals. Chromosome type is either autosome or sex
318 chromosome as assigned in Hmel2 reference genome (Davey *et al.*, 2016). 477
319 genes with no polymorphism were removed from the analysis. We plotted
320 diagnostic plots of residuals versus fitted values.

bioRxiv preprint doi: https://doi.org/10.1101/380030; this version posted July 31, 2018. The copyright holder for this preprint (which was not certified by peer review) is the author/funder, who has granted bioRxiv a license to display the preprint in perpetuity. It is made available under aCC-BY-NC-ND 4.0 International license.

Results

Hmel2.5 annotation and 1-1 orthologue prediction with *H. erato*

There are 20,118 transcripts predicted in *H. erato* (van Belleghem et al., 2017) and 20,097 genes (21,565 transcripts/proteins) in *H. melpomene* Hmel2.5. OrthoFinder returned 11,062 clusters of genes, 8085 of which included exactly one sequence per species. 14,841 (73.8%) of the total number of genes in H*. erato* were assigned to an orthogroup; and 14,857 (68.6%) of the total number of genes in *H. melpomene* version Hmel2.5 were assigned to an orthogroup (Supplementary Table S2). Conversely, the *H. melpomene* Hmel2 annotation has 13 019 predicted gene models (Davey *et al.*, 2016). Using the Hmel2 annotation, OrthoFinder returned 9,320 clusters of genes, 6846 of which included exactly one sequence per species (i.e. single-copy orthogroups). 13 744 (68.3%) genes were assigned to an orthogroup in *H. erato* and 10 530 (80.9%) were assigned to an orthogroup in *H. melpomene*. The Hmel2.5 annotation set for *H. melpomene* is therefore more comparable to the published *H. erato* gene annotation and is more appropriate for future gene-based analysis in *H. melpomene*. The Hmel2.5 annotation has 1,093 genes mapping to the Z chromosome and 18,835 mapping to the autosomes. This new version of *H. melpomene* genome annotation was numbered Hmel2.5 (available at LepBase http://ensembl.lepbase.org/Heliconius_melpomene_melpomene_hmel25/Info/Index , last accessed 20 Jun 2018, Challis *et al.*, BioRxiv preprint).

RNA-sequencing and read mapping

Analysis of gene expression profiles in the data retrieved from Walters *et al.* (2015) by principal component, the first principal component separates gene expression in whole abdomen by sex and explains 97% of variance (Supplementary Figure S1). The 25 *H. melpomene* samples sequenced for this

bioRxiv preprint doi: https://doi.org/10.1101/380030; this version posted July 31, 2018. The copyright holder for this preprint (which was not certified by peer review) is the author/funder, who has granted bioRxiv a license to display the preprint in perpetuity. It is made available under aCC-BY-NC-ND 4.0 International license.

project have a median total number of reads of 34.86 M (min. 27.81 M; max. 46.12 M), similar to previously published gene expression studies in *Heliconius* (Briscoe *et al.*, 2013; Walters *et al.*, 2015). Mapping success is high compared to other published studies (e.g. Yu et al., 2016 and Walters et al., 2015) (Supplementary Table S1). We analysed data from two different time points and from non-sex and sex-specific tissue separately (Treatment: Young and Old). There is a clear separation of the 25 samples by tissue when we compare gene expression profiles between them. In total, 51% of the total variance is explained by the two first principal components. PC1 separates the samples by tissue and explains 40% of variance. PC2 explains 11% of total variance and separates samples by age (Supplementary Figure S3). Ovarian tissue clusters by age more tightly than non-sex specific tissue (Gut) (Supplementary Figure S4A and S4B).

Coding sequence divergence does not support a significant fast-Z effect

We first compared rates of Z and autosomal sequence divergence using dN/dS comparisons of 1-1 orthologous genes between *H. melpomene* and *H. erato.* The dN/dS ratio for the Z chromosome genes is not significantly higher than dNdS for autosomal genes (dN/dS_{Auto}=0.110; 95% CI=[0.106-0.113]; dN/dS_Z=0.120; 95% CI= [0.098-0.145]), indicating no obvious faster Z divergence of coding sequence.

More highly expressed genes are more exposed to selection, so in a female heterogametic organism with a fast-Z effect, genes with female-biased expression are expected to have higher rates of amino acid substitution if dN/dS is driven by positive selection. However, the dN/dS ratio of Z female biased genes (dN/dS_Z=0.120; 95% CI=[0.069-0.183]) was not significantly different to that for male biased genes (dN/dS_Z=0.148 [0.122-0.172]) or unbiased genes ($dNdS_Z$=0.107; 95% CI=[0.078-0.143]). By contrast, among autosomal genes,

bioRxiv preprint doi: https://doi.org/10.1101/380030; this version posted July 31, 2018. The copyright holder for this preprint (which was not certified by peer review) is the author/funder, who has granted bioRxiv a license to display the preprint in perpetuity. It is made available under aCC-BY-NC-ND 4.0 International license.

those that are unbiased have a significantly lower coding sequence divergence compared to both male biased and female biased autosomal genes ($dNdS_Z$=0.0978; 95% CI=[0.093-0.102]) (Table 1).

Finally, dS on the Z chromosome (dS_Z=0.189; 95% CI= [0.18-0.2]) is higher than dS on the autosomes (dS_{Auto}=0.162; 95% CI= [0.16-0.17]), consistent with either a: 1) male-biased mutation rate, or 2) difference in coalescence time for autosomes and Z; but does not support a fast-Z effect (Table 1).

	Linkage	All	Female biased	Male biased	Unbiased
π_n/π_s	Autosomal	0.103 [0.100-0.107]	0.106 [0.10-0.113]	**0.127**$^{(A)}$ [0.118-0.138]	**0.094**$^{(A)}$ [0.091-0.098]
	Z	0.111 [0.098-0.126]	0.094 [0.059-0.136]	0.136 [0.112-0.162]	0.104 [0.09-0.125]
dN/dS	Autosomal	0.110 [0.106; 0.113]	0.113 [0.105; 0.121]	0.113 [0.145; 0.167]	**0.098**$^{(A)}$ [0.093; 0.102]
	Z	0.120 [0.098-0.145]	0.120 [0.069-0.183]	0.148 [0.122-0.172]	0.107 [0.078-0.143]
α ***Classic***	Autosomal	0.24 [-0.486-0.697]	0.120 [-0.54-0.687]	0.305 [-0.309-0.669]	0.225 [-0.544-0.719]
	Z	0.434 [-0.526-0.866]	0.463 [-0.276-0.837]	0.279 [-0.728-0.794]	0.535 [-0.475-1.0]

bioRxiv preprint doi: https://doi.org/10.1101/380030; this version posted July 31, 2018. The copyright holder for this preprint (which was not certified by peer review) is the author/funder, who has granted bioRxiv a license to display the preprint in perpetuity. It is made available under aCC-BY-NC-ND 4.0 International license.

Modeling	Autosomal	0.629 [0.622-0.636]	0.635 [0.620-0.650]	0.630 [0.616-0.646]	**0.538**$^{(B)}$ [0.529-0.547]
α	Z	**0.675**$^{(A)}$ [0.647-0.704]	0.699 [0.595-0.811]	0.646 [0.596-0.697]	**0.537**$^{(B)}$ [0.500-0.576]
	Autosomal	0.062 [0.061-0.063]	0.066 [0.065-0.068]	**0.087**$^{(B)}$ [0.085-0.089]	**0.047**$^{(B)}$ [0.046-0.048]
ω_a	Z	**0.069**$^{(A)}$ [0.066-0.072]	0.069 [0.058-0.080]	**0.090**$^{(B)}$ [0.083-0.097]	**0.048**$^{(B)}$ [0.044-0.051]
	Autosomal	0.036 [0.036-0.037]	0.038 [0.037-0.040]	**0.051**$^{(A)}$ [0.049-0.053]	0.040 [0.039-0.041]
ω_{na}	Z	0.033 [0.030-0.036]	0.029 [0.019-0.040]	0.049 [0.042-0.056]	0.041 [0.038-0.044]
#Genes	Autosomal	7464	1231	1238	4739
	Z	200	28	96	193

Table 1. Ratios of π_n/π_s, dN/dS; calculations of α, ω_a and ω_{na} for autosomal and Z male biased, female biased and unbiased genes

π_n/π_s, dN/dS ratios, α, ω_a and ω_{na} are shown for autosomal and Z male biased, female biased and unbiased genes. Intervals represent 95% confidence intervals obtained by bootstrapping 1,000 times. **Bold**$^{(A)}$

bioRxiv preprint doi: https://doi.org/10.1101/380030; this version posted July 31, 2018. The copyright holder for this preprint (which was not certified by peer review) is the author/funder, who has granted bioRxiv a license to display the preprint in perpetuity. It is made available under aCC-BY-NC-ND 4.0 International license.

391 denotes significant values within either Z or autosomal categories. **Bold**$^{(B)}$
392 denotes significant values within both Z and autosomal categories.
393 Significance indicated separately for *All* and for sex biased expression
394 (*female*, *male* & *unbiased*).

395

396 **π_{sZ}/π_{sA} diversity ratio is lower than 0.75**

397 We next explored patterns of within-species diversity as an indicator of the
398 strength of purifying selection. In a population at equilibrium with a 1:1 sex ratio
399 the π_{sZ}/π_{sA} diversity ratio is expected to be 0.75, but stronger purifying selection
400 on the Z chromosome would lead to a reduction in this ratio due to background
401 selection. The π_{sZ}/π_{sA} ratio for *H. melpomene* is approximately 0.44 (Table 2),
402 which might indicate purifying selection on the Z. However, this ratio can also be
403 influenced by a biased sex-ratio (Vicoso & Charlesworth, 2006), differences in
404 recombination rates (Charlesworth, 2012), sex-biased mutation rates (Vicoso &
405 Charlesworth, 2009), or a historical reduction in population size. Recent
406 calculations for *H. melpomene* from Panama using whole-genome short read
407 sequencing data estimated the π_{sZ}/π_{sA} diversity ratio value to be 0.611; CI=
408 [0.570-0.653] with only weak evidence for a population bottleneck (Van
409 Belleghem *et al.*, 2018). The more pronounced reduction in diversity at
410 synonymous sites we see here might therefore indicate enhanced background
411 selection in genic regions of the Z chromosome.

412

	Linkage	All	Female biased	Male biased	Unbiased
π_s	Autosomal	**0.027**$^{(A)}$ [0.026-0.027]	0.025 [0.024-0.027]	**0.035**$^{(A)}$ [0.033-0.036	0.025 [0.024-0.026]

bioRxiv preprint doi: https://doi.org/10.1101/380030; this version posted July 31, 2018. The copyright holder for this preprint (which was not certified by peer review) is the author/funder, who has granted bioRxiv a license to display the preprint in perpetuity. It is made available under aCC-BY-NC-ND 4.0 International license.

	Z	0.012 [0.011-0.013]	0.016 [0.013-0.020]	0.015 [0.01-0.02]	0.0106 [0.009-0.012]
π_{sZ}/π_{sA}	NA	0.444	NA	NA	NA

Table 2. *H. melpomene* π_s & π_{sZ}/π_{sA} ratio from pairwise alignments for Z and autosomal genes

π_s calculated from pairwise alignments for Z and autosomal genes. π_{sZ}/π_{sA} ratio used to estimate N_{eZ}/N_{eA}. Intervals represent 95% confidence intervals obtained by bootstrapping genes (1000 replicates). **Bold** [(A)] denotes significant values within either Z or autosomal categories. Significance indicated separately for *All* and for sex biased (*female*, *male* & *unbiased*).

Increased strength of purifying selection on highly expressed genes

Patterns of diversity were however strongly associated with expression levels. Using a multiple regression approach we found that functional genetic diversity, $\pi_{n,}$ was significantly negatively correlated with expression level for both autosomal ($P < 0.01$) consistent with increased purifying selection on highly expressed genes (Supplementary Figure S2).

bioRxiv preprint doi: https://doi.org/10.1101/380030; this version posted July 31, 2018. The copyright holder for this preprint (which was not certified by peer review) is the author/funder, who has granted bioRxiv a license to display the preprint in perpetuity. It is made available under aCC-BY-NC-ND 4.0 International license.

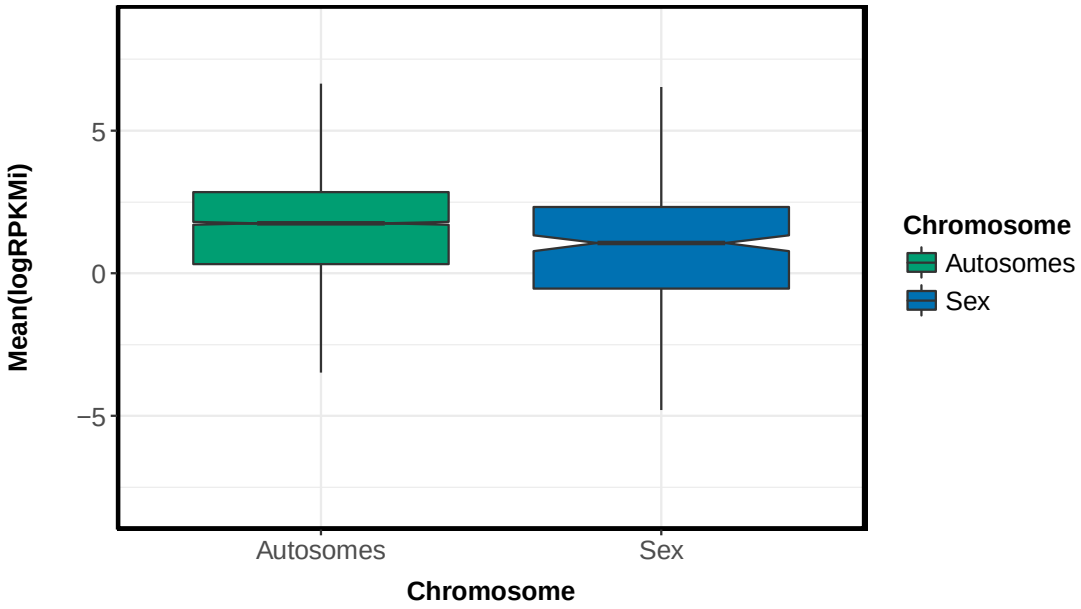

Figure 1. Expression level of Z and autosomal genes

Median expression level of Z genes is significantly lower than autosomal genes ($P < 0.05$). Notches on boxplot display the confidence intervals around the median.

Z and autosomal rates of adaptive substitution: testing fast-Z adaptation

We next explored patterns of adaptive evolution using: 1) the *Classic* MK test; and 2) the *Modelling* approach which accounts for the effect of mildly deleterious mutations. We computed: 1) the proportion of adaptive non-synonymous substitutions (α) for both the *Classic* and the *Modelling* approaches; and 2) ω_a and ω_{na} for the *Modelling approach*. ω_a is the per mutation rate of adaptive substitutions and ω_{na} is the per mutation rate of non-adaptive substitutions.

There are no significant differences in α values between gene categories under the *Classic approach* (Table 1). However, using the *Modelling approach*, when all genes are considered, Z genes have a marginally but significantly higher α (α_Z=0.675; 95% CI= [0.647-0.704]) than those that are autosomal (α_{Auto}=0.629;

bioRxiv preprint doi: https://doi.org/10.1101/380030; this version posted July 31, 2018. The copyright holder for this preprint (which was not certified by peer review) is the author/funder, who has granted bioRxiv a license to display the preprint in perpetuity. It is made available under aCC-BY-NC-ND 4.0 International license.

95% CI= [0.622-0.636]). Nonetheless, α is not significantly different between the Z chromosome and autosomes for female biased (α_{Auto}=0.635; 95% CI= [0.62-0.65]; α_Z=0.699; 95% CI= [0.595-0.811]) or male biased genes (α_{Auto}=0.63; 95% CI= [0.616-0.646]; α_Z=0.646; 95% CI= [0.596-0.697]). Unbiased genes have significantly lower α values than female or male biased genes for both Z and autosomes, but within the unbiased genes there is no significant difference in α between Z (α_Z=0.537; 95% CI= [0.5-0.567]) and autosomes (α_{Auto}=0.538; 95% CI= [0.529-0.547]) (Table 1). The lack of significant differences in α between sex-biased genes is not consistent with the expectations of fast-Z adaptation, which would predict faster evolution of female biased genes due to hemizygosity compared to autosomes, but this could also reflect a lack of power to detect the signal when the total number of genes is reduced.

Hemizygosity and the rate of adaptive substitutions

Similarly, ω_α, the rate of adaptive substitution relative to the rate of neutral divergence, is significantly higher for Z genes ($\omega_{\alpha Z}$=0.069; 95% CI= [0.066-0.072])as compared to autosomal genes ($\omega_{\alpha Auto}$=0.062; 95% CI= [0.061-0.063]), consistent with the hypothesis of faster-Z evolution. However, contrary to the prediction for faster-Z evolution, ω_α is significantly higher for both male biased autosomal ($\omega_{\alpha\ Auto}$=0.087; 95% CI= [0.085-0.089]) and Z genes ($\omega_{\alpha\ Z}$=0.090; 95% CI= [0.083-0.097]) as compared to for female biased genes ($\omega_{\alpha\ Z}$=0.069; 95% CI= [0.058-0.08]; $\omega_{\alpha\ Auto}$=0.066; 95% CI= [0.065-0.068]). ω_α is significantly lower for unbiased genes as compared to male and female biased genes, both in autosomal ($\omega_{\alpha\ Auto}$=0.047; 95% CI= [0.046-0.048]) and sex chromosome $\omega_{\alpha\ Z}$=0.048; 95% CI= [0.044-0.051]).

bioRxiv preprint doi: https://doi.org/10.1101/380030; this version posted July 31, 2018. The copyright holder for this preprint (which was not certified by peer review) is the author/funder, who has granted bioRxiv a license to display the preprint in perpetuity. It is made available under aCC-BY-NC-ND 4.0 International license.

There was no evidence for reduced purifying selection on the Z chromosome, as the per-mutation rate of non-adaptive substitution ($\omega_{n\alpha}$) is lower for Z genes ($\omega_{n\alpha Z}$ =0.033; 95% CI= [0.030-0.036] and $\omega_{n\alpha\ Auto}$=0.036; 95% CI= [0.036-0.037]). Female biased genes have the lowest $\omega_{n\alpha}$ ($\omega_{n\alpha\ Auto}$=0.038; 95% CI= [0.037-0.040]; $\omega_{n\alpha\ Z}$=0.029; 95% CI= [0.019-0.040]) compared to male biased ($\omega_{n\alpha\ Auto}$=0.051; 95% CI= [0.049-0.053]; $\omega_{n\alpha\ Z}$=0.049; 95% CI= [0.042-0.056]) and unbiased ($\omega_{n\alpha\ Auto}$=0.04; 95% CI= [0.039-0.041]; $\omega_{n\alpha\ Z}$=0.041; 95% CI= [0.038-0.044]) genes, which confirms the low π_n/π_s already reported and would suggest that purifying selection is stronger in female biased genes.

Female ovary-biased and gut-biased genes

Next we explored the expression of genes in female reproductive tissue. Overall there were a greater number of genes with gut-biased expression (#Gut_{Auto}=153) than ovary biased expression (#$Ovary_{Auto}$=40) in the autosomes. However, there was an over-representation of Z ovary expressed genes than expected by chance (#Gut_Z=6; #$Ovary_Z$=6; chi-square test; $P < 0.05$). However, the number of genes in each category is relatively small so these tests should be treated with caution.

Of the 205 differentially expressed genes between the two tissues only 9 in the ovaries and 26 in the gut could be used to calculate dN/dS, π_n/π_s and α. The other genes either do not have a 1-1 ortholog with *H. erato* or there were too many undetermined characters (gaps or Ns) to be able to estimate the parameters. Of the 35 genes for which molecular evolution statistics could be calculated, all 9 ovary biased and 25 of 26 gut biased genes are autosomal; and 1 gut biased gene maps to the Z (Gut dN/dS_Z=0.365; Gut $\pi_n/\pi_{s\ Z}$=0.093; Gut α_Z=0.295). We did not detect any significant differences in π_n/π_s; dN/dS; or α for autosomal ovary and gut-biased genes.

bioRxiv preprint doi: https://doi.org/10.1101/380030; this version posted July 31, 2018. The copyright holder for this preprint (which was not certified by peer review) is the author/funder, who has granted bioRxiv a license to display the preprint in perpetuity. It is made available under aCC-BY-NC-ND 4.0 International license.

Discussion

Elevated rates of coding sequence evolution on the sex chromosome relative to autosomes have been reported for several species, consistent with the theoretical prediction of fast-X evolution. Here we find evidence for enhanced rates of adaptation on the *Heliconius* Z chromosome: Z genes have a significantly higher rate of adaptive evolution when all expressed genes are considered. However, fast-X theory predicts that genes highly expressed in the hemizygous sex should be especially prone to fast-X evolution, but this prediction was not fulfilled in our data. Female-biased genes were not more fast evolving when located on the Z chromosome. The evidence for fast-Z evolution in *Heliconius* is therefore somewhat mixed.

In other taxa there is strongest support for fast-X evolution in groups with complete dosage compensation (Mank, Vicoso, *et al.*, 2010; Meisel and Connallon, 2013). Theory predicts that opportunities for fast-X evolution should increase in species with somatic X-inactivation such as eutherian mammals, as there is effectively haploid expression of the sex chromosome in cells, increasing the chances of recessive beneficial mutations being fixed (Charlesworth *et al.*, 1987). Groups such as Lepidoptera have been reported to have more complex patterns of sex chromosome dosage compensation. In *Heliconius* males expression of Z genes is reduced below autosomal levels, but this dosage compensation mechanism is imperfect, with males showing increased expression relative to females on the Z chromosome (Walters *et al.*, 2015). However, alternative processes, such as the masculinization of the Z chromosome, may explain the apparent lack of complete dosage compensation (Gu & Walters, 2017, Huylmans *et al.* 2017). Regardless, when we compare rates of divergence and adaptation for genes with sex-biased expression, the expectations of fast-Z evolution are not clearly met. While we might expect faster rates of adaptive evolution for female-biased genes, in fact there is a weak tendency for faster rates of evolution in male-biased genes.

bioRxiv preprint doi: https://doi.org/10.1101/380030; this version posted July 31, 2018. The copyright holder for this preprint (which was not certified by peer review) is the author/funder, who has granted bioRxiv a license to display the preprint in perpetuity. It is made available under aCC-BY-NC-ND 4.0 International license.

Although a fast-Z effect has been observed in *Bombyx mori* (Sackton *et al.*, 2014), no such pattern was reported in two satyrine butterflies where the dN/dS ratio of Z genes was slightly lower than for autosomal genes (Rousselle *et al.*, 2016). In *Heliconius*, although dN/dS was not significantly different between autosomal and Z genes, we did find evidence for a faster rate of adaptive substitution. Interestingly, our data also show that dS on the Z chromosome is higher than dS on the autosomes perhaps indicating a male biased mutation rate, as Z chromosomes spend more time in males than in females (Miyata *et al.*, 1987). While hemizygosity is expected to expose beneficial mutations to selection and increase rates of adaptive evolution on the Z chromosome, it is also expected to increase the efficacy of purifying selection which would act to reduce evolutionary rates. It may be that the balance between these two forces differs across lepidopteran species, leading to the mixed pattern of fast-Z evolution in some taxa but not others. It is important to add, however, that the α values estimated in this study are substantially higher than α reported in Martin *et al*. (2016). Martin *et al.* (2016) estimated α using the approach developed by Messer & Petrov (2013) and, in simulations, it has been shown that it is possible that there is an overestimation of DFE-α (the method used in this study) in scenarios with strong sweeps or population expansion (Messer and Petrov, 2013).

Wright *et al*. (2015) interpreted the high dN/dS in Z genes of birds as a consequence of reduced effective population size rather than positive selection. The difference in effective population size between sex chromosomes and autosomes in female heterogametic systems is predicted to be larger than in male heterogametic systems due to higher variance of male reproductive success (Mank, Nam, *et al.*, 2010). Indeed, we estimate that coding regions on the Z chromosome have an N_e 0.44 times that of autosomes. We might therefore predict a considerable reduction in the efficacy of purifying selection on butterfly Z chromosomes. This should lead to higher ω_{na} and π_n/π_s ratios on the Z compared due to stronger genetic drift. However, as in satyrine butterflies

bioRxiv preprint doi: https://doi.org/10.1101/380030; this version posted July 31, 2018. The copyright holder for this preprint (which was not certified by peer review) is the author/funder, who has granted bioRxiv a license to display the preprint in perpetuity. It is made available under aCC-BY-NC-ND 4.0 International license.

(Rousselle *et al.*, 2016), in *Heliconius*, ω_{na} is not higher on the Z relative to autosomes. dN/dS and π_n/π_s are higher in the Z relative to autosomes in *Heliconius*, but this is not significant. This means that, in contrast to birds, the difference in the effective population size of the Z relative to autosomes is not sufficient to reduce the efficacy of purifying selection at a detectable level.

One possible explanation for this difference is the generally much higher effective population sizes of Lepidoptera, which could allow for efficient selection even on sex chromosome (Rousselle *et al.*, 2016). Another is that by not using all genomic sites to estimate the π_{sZ}/π_{sA} diversity ratio, we might be underestimating its true value due to a stronger effect of background selection. The latter is supported by the observation that, in a recently published paper using all genomic sites to estimate π_{sZ}/π_{sA}, Van Belleghem *et al.* (2018) calculated it to be 0.661 CI= [0.570-0.653]. Regardless both ours and Van Belleghem *et al.* (2018) estimates of the π_{sZ}/π_{sA} diversity ratio are significantly lower than the expected 0.75 and still there is no observable reduction in the efficacy of purifying selection in *H. melpomene*.

Another factor that might counteract the fast-Z effect is adaptation from standing variation. Larger populations are more polymorphic and therefore have an increased probability of adaption from standing genetic variation. Adaptation from standing genetic variation is therefore expected to result in faster-autosome evolution, independent of the dominance of beneficial alleles (Orr and Betancourt, 2001), which would counteract the fast-Z effect. This may be especially relevant when overall population sizes are large, as in many *Heliconius* species, such that standing variation becomes a comparatively important source of adaptive variation as compared to *de novo* mutations.

As sex biased genes tend to be expressed in sex specific tissue such as the testis and the ovaries we aimed to investigate patterns of molecular evolution in ovary biased genes. Unfortunately, there are no ovary-biased genes with 1-1 orthologues between *H. melpomene* and *H. erato* that are Z. This means we

bioRxiv preprint doi: https://doi.org/10.1101/380030; this version posted July 31, 2018. The copyright holder for this preprint (which was not certified by peer review) is the author/funder, who has granted bioRxiv a license to display the preprint in perpetuity. It is made available under aCC-BY-NC-ND 4.0 International license.

593 could not test the effect of hemizygosity on non-sex specific and sex-specific
594 female expression directly. The lack of 1-1 orthology may mean that these genes
595 are rapidly evolving, and indeed autosomal ovary-expressed genes do have
596 higher rates of adaptive evolution than gut expressed genes.

597 Together these results illustrate the need to study substitution rates in other ZW
598 systems considering sex biased expression. This genome-wide analysis of
599 polymorphism, divergence and gene expression data contributes to a growing
600 body of literature on sex chromosome evolution in ZW systems, and reveals the
601 complexity of the different evolutionary forces shaping transcriptome evolution in
602 *Heliconius* and, consistent with previous work, shows limited evidence of fast-Z
603 evolution in this taxon.

604 **References**

605

606 Anders S, Pyl PT, Huber W (2015). HTSeq--a Python framework to work with
607 high-throughput sequencing data. Bioinformatics 31: 166–169.
608
609 Assis R, Zhou Q, Bachtrog D (2012). Sexbiased transcriptome evolution in
610 Drosophila. Genome Biology and Evolution 4: 1189–1200.
611
612 Avila V, Procé SM, Campos JL, Borthwick H, Charlesworth B, Betancourt AJ;
613 Faster-X Effects in Two Drosophila Lineages, Genome Biology and
614 Evolution, Volume 6, Issue 10, 1 October 2014, Pages 2968–2982.
615
616 Avila V, Campos JL, Charlesworth B (2015). The effects of sex biased gene
617 expression and X-linkage on rates of adaptive protein sequence evolution in
618 Drosophila. Biology Letters 11: 20150117–20150117.
619
620 Baines JF, Harr B (2007). Reduced X-linked diversity in derived populations of
621 house mice. Genetics 175: 1911–1921.

bioRxiv preprint doi: https://doi.org/10.1101/380030; this version posted July 31, 2018. The copyright holder for this preprint (which was not certified by peer review) is the author/funder, who has granted bioRxiv a license to display the preprint in perpetuity. It is made available under aCC-BY-NC-ND 4.0 International license.

622 Bao W, Kojima KK, Kohany O (2015). Repbase Update, a database of repetitive
623 elements in eukaryotic genomes. Mob DNA, 6:11

624 Briscoe AD, Macias-Muñoz A, Kozak KM, Walters JR, Yuan F, Jamie GA, et al.
625 (2013). Female behaviour drives expression and evolution of gustatory
626 receptors in butterflies. (J Zhang, Ed.). PLoS Genet 9: e1003620.
627
628 Bustamante CD et al. (2005). Natural selection on protein-coding genes in the
629 human genome. Nature, 437(7062), pp.1153 EP —1157.
630
631 Carneiro M, Albert FW, Melo-Ferreira J, Galtier N, Gayral P, Blanco-Aguiar JA, et
632 al. (2012). Evidence for widespread positive and purifying selection across
633 the European rabbit (Oryctolagus cuniculus) genome. Molecular Biology and
634 Evolution 29: 1837–1849.
635
636 Charlesworth, B (2012). The role of background selection in shaping patterns of
637 molecular evolution and variation: evidence from variability on the Drosophila
638 X chromosome. Genetics, 191(1), 233–246.
639
640 Connallon T, Singh ND, Clark AG (2012). Impact of genetic architecture on the
641 relative rates of X versus autosomal adaptive substitution. Molecular Biology
642 and Evolution 29: 1933–1942.
643
644 Cox RM, Cox CL, McGlothlin JW, Card DC, Andrew AL, Castoe TA (2017).
645 Hormonally Mediated Increases in Sexbiased Gene Expression Accompany
646 the Breakdown of Between-Sex Genetic Correlations in a Sexually Dimorphic
647 Lizard. Am Nat 189: 315–332.
648
649 Davey JW, Chouteau M, Barker SL, Maroja L, Baxter SW, Simpson F, et al.
650 (2016). Major Improvements to the Heliconius melpomene Genome
651 Assembly Used to Confirm 10 Chromosome Fusion Events in 6 Million Years

bioRxiv preprint doi: https://doi.org/10.1101/380030; this version posted July 31, 2018. The copyright holder for this preprint (which was not certified by peer review) is the author/funder, who has granted bioRxiv a license to display the preprint in perpetuity. It is made available under aCC-BY-NC-ND 4.0 International license.

652 of Butterfly Evolution. G3 6: 695-708.
653
654 De Mita S, Siol M (2012). EggLib: processing, analysis and simulation tools for
655 population genetics and genomics. BMC Genet 13: 27.
656
657 DePristo MA, Banks E, Poplin R, Garimella KV, Maguire JR, Hartl C, et al.
658 (2011). A framework for variation discovery and genotyping using next-
659 generation DNA sequencing data. Nature Publishing Group 43: 491–498.
660
661 Dutheil J, Boussau B (2008). Non-homogeneous models of sequence evolution
662 in the Bio++ suite of libraries and programs. BMC Evolutionary Biology 8:
663 255.

664 Fay JC (2011) Weighing the evidence for adaptation at the molecular level. *Trends Genet*
665 *27(9):*343–349.

666 Ellegren H, Parsch J (2007). The evolution of sexbiased genes and sexbiased
667 gene expression. Nat Rev Genet 8: 689–698.
668
669 Galtier N (2016). Adaptive Protein Evolution in Animals and the Effective
670 Population Size Hypothesis. (MH Schierup, Ed.). PLoS Genet 12: e1005774.
671
672 Grath S, Parsch J (2016). Sex biased Gene Expression. Annu Rev Genet 50:
673 29–44.
674
675 Hoff KJ, Lange S, Lomsadze A, Borodovsky M, & Stanke M (2016). BRAKER1:
676 Unsupervised RNA-Seq-Based Genome Annotation with GeneMark-ET and
677 AUGUSTUS. Bioinformatics, 32(5), 767–769.
678
679 Hu TT, Eisen MB, Thornton KR, Andolfatto P (2013). A second-generation
680 assembly of the Drosophila simulans genome provides new insights into
681 patterns of lineage-specific divergence. Genome Research 23: 89–98.

bioRxiv preprint doi: https://doi.org/10.1101/380030; this version posted July 31, 2018. The copyright holder for this preprint (which was not certified by peer review) is the author/funder, who has granted bioRxiv a license to display the preprint in perpetuity. It is made available under aCC-BY-NC-ND 4.0 International license.

Huylmans AK, Macon A, Vicoso B (2017). Global Dosage Compensation Is Ubiquitous in Lepidoptera, but Counteracted by the Masculinization of the Z Chromosome., 34 (10), 2637–2649.

Kim D, Langmead B, Salzberg SL (2015). HISAT: a fast spliced aligner with low memory requirements. Nat Meth 12: 357–360.

Kirkpatrick M, Hall DW (2004). Malebiased mutation, sex linkage, and the rate of adaptive evolution. Evolution 58: 437–440.

Kozak KM, Wahlberg N, Neild AFE, Dasmahapatra KK, Mallet J, & Jiggins CD (2015). Multilocus species trees show the recent adaptive radiation of the mimetic *Heliconius* butterflies. Systematic Biology, 64(3), 505–524.

Li H, Durbin R (2009). Fast and accurate short read alignment with Burrows-Wheeler transform. Bioinformatics 25: 1754–1760.

Li H, Handsaker B, Wysoker A, Fennell T, Ruan J, Homer N, et al. (2009). The Sequence Alignment/Map format and SAMtools. Bioinformatics 25: 2078–2079.

Love MI, Huber W, Anders S (2014). Moderated estimation of fold change and dispersion for RNA-seq data with DESeq2. 15: 550.

Mackay TFC, Richards S, Stone EA, Barbadilla A, Ayroles JF, Zhu D, et al. (2012). The Drosophila melanogaster Genetic Reference Panel. Nature 482: 173–178.

Mank JE, Nam K, Ellegren H (2010). Faster-Z evolution is predominantly due to genetic drift. Molecular Biology and Evolution 27: 661–670.

bioRxiv preprint doi: https://doi.org/10.1101/380030; this version posted July 31, 2018. The copyright holder for this preprint (which was not certified by peer review) is the author/funder, who has granted bioRxiv a license to display the preprint in perpetuity. It is made available under aCC-BY-NC-ND 4.0 International license.

Mank JE, Vicoso B, Berlin S, Charlesworth B (2010). Effective population size and the Faster-X effect: empirical results and their interpretation. Evolution 64: 663–674.

Mank JE, & Ellegren H (2009). Are sex-biased genes more dispensable? Biology Letters, 5(3), 409–412.

Martin SH, Möst M, Palmer WJ, Salazar C, McMillan WO, Jiggins FM, & Jiggins CD (2016). Natural Selection and Genetic Diversity in the Butterfly Heliconius melpomene. Genetics, 203(1), 525–541.

Macpherson M, Sella G, Davis JC, and Petrov DA (2007) Genome-wide spatial correspondence between non-synonymous divergence and neutral polymorphism reveals extensive adaptation in Drosophila. Genetics 177: 2083-89.

McDonald JH, Kreitman M (1991). Adaptive protein evolution at the Adh locus in Drosophila. Nature 351: 652–654.

Meisel RP, Connallon T (2013). The faster-X effect: integrating theory and data. Trends in Genetics 29: 537–544.

Meisel RP, Malone JH, Clark AG (2012). Faster-X evolution of gene expression in Drosophila. (D Bachtrog, Ed.). PLoS Genet 8: e1003013.

Messer PW, & Petrov DA (2013). Frequent adaptation and the McDonald-Kreitman test. Proceedings of the National Academy of Sciences of the United States of America, 110(21), 8615–8620.

Miyata T, Hayashida H, Kuma K, Mitsuyasu K, Yasunaga T (1987). Male-driven

bioRxiv preprint doi: https://doi.org/10.1101/380030; this version posted July 31, 2018. The copyright holder for this preprint (which was not certified by peer review) is the author/funder, who has granted bioRxiv a license to display the preprint in perpetuity. It is made available under aCC-BY-NC-ND 4.0 International license.

744 molecular evolution: a model and nucleotide sequence analysis. Cold Spring
745 Harb Symp Quant Biol 52: 863–867.
746
747 Mortazavi A, Williams BA, McCue K, Schaeffer L, & Wold B (2008). Mapping and
748 quantifying mammalian transcriptomes by RNA-Seq. Nature Methods, 5(7),
749 621–628.
750
751 Nam K, Munch K, Hobolth A, Dutheil JY, Veeramah KR, Woerner AE, et al.
752 (2015). Extreme selective sweeps independently targeted the X
753 chromosomes of the great apes. Proc Natl Acad Sci USA 112: 6413–6418.
754
755 Nielsen R, Bustamante C, Clark AG, Glanowski S, Sackton TB, Hubisz MJ, et al.
756 (2005). A scan for positively selected genes in the genomes of humans and
757 chimpanzees. (C Tyler-Smith, Ed.). PLoS Biol 3: e170.
758
759 O'Neill MB, Mortimer TD, Pepperell CS (2015). Diversity of Mycobacterium
760 tuberculosis across Evolutionary Scales. (SM Fortune, Ed.). PLoS Pathog 11:
761 e1005257.
762
763 Orr HA (2010). The population genetics of beneficial mutations. Philos Trans R
764 Soc Lond, B, Biol Sci 365: 1195–1201.
765
766 Orr HA, Betancourt AJ (2001). Haldane's sieve and adaptation from the standing
767 genetic variation. Genetics 157: 875–884.
768
769 Parisi M, Nuttall R, Edwards P, Minor J, Naiman D, Lü J, et al. (2004). A survey
770 of ovary, testis-, and soma biased gene expression in Drosophila
771 melanogaster adults. 5: R40.
772
773 Parisi M, Nuttall R, Naiman D, Bouffard G, Malley J, Andrews J, et al. (2003).
774 Paucity of genes on the Drosophila X chromosome showing malebiased

bioRxiv preprint doi: https://doi.org/10.1101/380030; this version posted July 31, 2018. The copyright holder for this preprint (which was not certified by peer review) is the author/funder, who has granted bioRxiv a license to display the preprint in perpetuity. It is made available under aCC-BY-NC-ND 4.0 International license.

expression. Science 299: 697–700.

Pool JE and Nielsen R (2007). Population size changes reshape genomic patterns of diversity. Evolution 61(12), pp.3001–3006.

Van Belleghem SM, Baquero M, Papa R, et al. Patterns of Z chromosome divergence among *Heliconius*species highlight the importance of historical demography. Mol Ecol. 2018; 00:1–21.

Ranwez V, Harispe S, Delsuc F, Douzery EJP (2011). MACSE: Multiple Alignment of Coding SEquences accounting for frameshifts and stop codons. (WJ Murphy, Ed.). PLoS ONE 6: e22594.

Rastogi A, Gupta D (2014). GFF-Ex: a genome feature extraction package. BMC Res Notes 7: 315.

Rice WR (1984). Sex chromosomes and the evolution of sexual dimorphism. Evolution 38: 735–742.

Rousselle M, Faivre N, Ballenghien M, Galtier N, Nabholz B (2016). Hemizygosity Enhances Purifying Selection: Lack of Fast-Z Evolution in Two Satyrine Butterflies. Genome Biology and Evolution 8: 3108–3119.

Sackton TB, Corbett-Detig RB, Nagaraju J, Vaishna L, Arunkumar KP, Hartl DL (2014). Positive selection drives faster-Z evolution in silkmoths. Evolution 68: 2331–2342.

Sella G, Petrov DA, Przeworski M, & Andolfatto P (2009). Pervasive natural selection in the Drosophila genome? PLoS Genetics, 5(6), e1000495.

Thornton K, Bachtrog D, Andolfatto P (2006). X chromosomes and autosomes evolve at similar rates in Drosophila: no evidence for faster-X protein

bioRxiv preprint doi: https://doi.org/10.1101/380030; this version posted July 31, 2018. The copyright holder for this preprint (which was not certified by peer review) is the author/funder, who has granted bioRxiv a license to display the preprint in perpetuity. It is made available under aCC-BY-NC-ND 4.0 International license.

evolution. Genome Research 16: 498–504.

Thornton K, Long M (2002). Rapid divergence of gene duplicates on the Drosophila melanogaster X chromosome. Molecular Biology and Evolution 19: 918–925.

Vicoso B, Charlesworth B (2006). Evolution on the X chromosome: unusual patterns and processes. Nat Rev Genet 7: 645–653.

Vicoso B, Charlesworth B (2009). Effective population size and the faster-X effect: an extended model. Evolution 63: 2413–2426.

Walters JR, Hardcastle TJ, Jiggins CD (2015). Sex Chromosome Dosage Compensation in Heliconius Butterflies: Global yet Still Incomplete? Genome Biology and Evolution 7: 2545–2559.

Wright AE, Zimmer F, Harrison PW, Mank JE (2015). Conservation of Regional Variation in Sex-Specific Sex Chromosome Regulation. Genetics 201(2): 587–598.

Zhang Z, Hambuch TM, Parsch J (2004). Molecular evolution of sex biased genes in Drosophila. Molecular Biology and Evolution 21: 2130–2139.

Zhang L and Li WH. (2005). Human SNPs reveal no evidence of frequent positive selection. *Molecular Biology and Evolution*, *22*(12), 2504–2507.

Zhou Q, Bachtrog D (2012). Sex-specific adaptation drives early sex chromosome evolution in Drosophila. Science 337: 341–345.

bioRxiv preprint doi: https://doi.org/10.1101/380030; this version posted July 31, 2018. The copyright holder for this preprint (which was not certified by peer review) is the author/funder, who has granted bioRxiv a license to display the preprint in perpetuity. It is made available under aCC-BY-NC-ND 4.0 International license.

Supplementary Tables

- **Supplementary Table S1**. Sample information and statistics

- **Supplementary Table S2.** Orthologue prediction improvement with Hmel2.5 annotation

- **Supplementary Table S3.** Mean and median read-depth for resequenced whole-genome *H. melpomene* samples (van Belleghem *et al.*, 2018)

bioRxiv preprint doi: https://doi.org/10.1101/380030; this version posted July 31, 2018. The copyright holder for this preprint (which was not certified by peer review) is the author/funder, who has granted bioRxiv a license to display the preprint in perpetuity. It is made available under aCC-BY-NC-ND 4.0 International license.

858

859

860 **Supplementary Table S1. Sample information and statistics**

Sample	Sex	Tissue	Treatment	Library	Raw Reads
AP141	Female	Gut	Old	RRB03031	32306468
AP93	Female	Gut	Young	RRB03025	34353682
AP142	Female	Gut	Old	RRB03032	34445514
AP77	Female	Gut	Old	RRB03030	32024898
AP89	Female	Gut	Old	RRB03034	39661158
AP55	Female	Gut	Old	RRB03035	35862378
AP94	Female	Gut	Young	RRB03026	36223403
AP37	Female	Gut	Young	RRB03029	31187077
AP34	Female	Gut	Young	RRB03028	35452206
AP71	Female	Gut	Young	RRB03024	33088963
AP35	Female	Gut	Young	RRB03027	46122142
AP80	Female	Gut	Old	RRB03033	40040750
AP35	Female	Ovaries	Young	RRBL00006	35018481
AP94	Female	Ovaries	Young	RRB02962	39903075
AP34	Female	Ovaries	Young	RRB02963	27811550
AP37	Female	Ovaries	Young	RRB02960	33410348
AP71	Female	Ovaries	Young	RRBL00007	34856038
AP88	Female	Ovaries	Young	RRBL00008	38486006
AP93	Female	Ovaries	Young	RRB02961	31497198
AP55	Female	Ovaries	Old	RRB03012	37934077
AP77	Female	Ovaries	Old	RRB03013	34322656
AP80	Female	Ovaries	Old	RRB03014	36157750
AP89	Female	Ovaries	Old	RRB03015	34318423
AP141	Female	Ovaries	Old	RRB03016	33844256
AP142	Female	Ovaries	Old	RRB03017	35328097
R20	Female	Abdomen	Young	NA	NA
R29	Female	Abdomen	Young	NA	NA
R06	Male	Abdomen	Young	NA	NA
R32	Male	Abdomen	Young	NA	NA
R34	Male	Abdomen	Young	NA	NA
R07	Female	Abdomen	Young	NA	NA
R33	Male	Abdomen	Young	NA	NA
R05	Female	Abdomen	Young	NA	NA
R21	Male	Abdomen	Young	NA	NA
R28	Female	Abdomen	Young	NA	NA

bioRxiv preprint doi: https://doi.org/10.1101/380030; this version posted July 31, 2018. The copyright holder for this preprint (which was not certified by peer review) is the author/funder, who has granted bioRxiv a license to display the preprint in perpetuity. It is made available under aCC-BY-NC-ND 4.0 International license.

861

862

863 **Supplementary Table S1. Sample information and statistics (cont.)**

Sample	Raw Base (G)	Error Rate (%)	Q20 (%)	Q30 (%)	GC content (%)
AP141	9.69	0.01	98.25	95.7	41.52
AP93	10.31	0.01	97.38	93.98	40.89
AP142	10.33	0.01	98.25	95.75	41.5
AP77	9.61	0.01	98.23	95.69	42.14
AP89	11.9	0.01	98.11	95.53	42.53
AP55	10.76	0.01	98.15	95.6	41.52
AP94	10.87	0.01	97.94	95.03	41.41
AP37	9.36	0.01	98.52	96.42	42.95
AP34	10.64	0.01	98.53	96.4	41.49
AP71	9.93	0.01	98.12	95.39	40.62
AP35	13.84	0.01	97.84	94.81	40.47
AP80	12.01	0.01	98.19	95.62	42
AP35	10.51	0.01	98.53	96.41	41.08
AP94	11.97	0.01	98.16	95.19	41.51
AP34	8.34	0.01	98.2	95.27	41.42
AP37	10.02	0.01	98.49	95.88	42.15
AP71	10.46	0.01	98.42	96.19	41.36
AP88	11.55	0.01	98.53	96.37	42.71
AP93	9.45	0.01	98.38	95.69	41.24
AP55	11.38	0.01	98.17	95.51	39.76
AP77	10.3	0.01	98.28	95.6	40.46
AP80	10.85	0.01	97.97	95.06	40.28
AP89	10.3	0.01	98.04	95.16	41.51
AP141	10.15	0.01	97.88	94.83	39.58
AP142	10.6	0.01	98	95.09	39.69
R20	NA	NA	NA	NA	NA
R29	NA	NA	NA	NA	NA
R06	NA	NA	NA	NA	NA
R32	NA	NA	NA	NA	NA
R34	NA	NA	NA	NA	NA
R07	NA	NA	NA	NA	NA
R33	NA	NA	NA	NA	NA
R05	NA	NA	NA	NA	NA
R21	NA	NA	NA	NA	NA
R28	NA	NA	NA	NA	NA

bioRxiv preprint doi: https://doi.org/10.1101/380030; this version posted July 31, 2018. The copyright holder for this preprint (which was not certified by peer review) is the author/funder, who has granted bioRxiv a license to display the preprint in perpetuity. It is made available under aCC-BY-NC-ND 4.0 International license.

Supplementary Table S1. Sample information and statistics (cont.)

Sample	Mapped Reads(%)	Properly Paired(%)
AP141	83.40	78.16
AP93	75.27	69.38
AP142	79.84	74.32
AP77	79.71	74.03
AP89	73.41	67.05
AP55	77.95	72.08
AP94	62.79	58.07
AP37	76.98	72.13
AP34	81.84	76.85
AP71	79.86	74.15
AP35	76.68	71.58
AP80	75.17	69.39
AP35	76.76	71.96
AP94	82.03	77.30
AP34	86.45	81.59
AP37	83.17	78.42
AP71	85.70	80.81
AP88	86.99	82.85
AP93	82.80	78.53
AP55	85.29	80.51
AP77	87.83	83.17
AP80	86.56	81.74
AP89	85.34	80.68
AP141	88.09	83.44
AP142	87.19	82.62
R20	38.20	34.46
R29	31.92	29.07
R06	60.95	53.47
R32	85.00	77.32
R34	29.08	26.05
R07	83.25	76.15
R33	35.84	30.56
R05	71.44	64.81
R21	38.06	31.36
R28	61.37	54.10

bioRxiv preprint doi: https://doi.org/10.1101/380030; this version posted July 31, 2018. The copyright holder for this preprint (which was not certified by peer review) is the author/funder, who has granted bioRxiv a license to display the preprint in perpetuity. It is made available under aCC-BY-NC-ND 4.0 International license.

867

868

869 **Supplementary Table S1. Sample information and statistics**

870 *H. melpomene rosina* RNA-seq mapping statistics. Sample ID, species,
871 tissue, stage of collection for mRNA 150bp PE directionally sequenced
872 reads for this project. Samples mapped to *H. melpomene* genome v2.1.
873 Walters *et al.* (2015) sample mapping statistics to *H. melpomene* genome
874 v2.1.

875

876

877

878

879

880

881

882

883

884

885

886

bioRxiv preprint doi: https://doi.org/10.1101/380030; this version posted July 31, 2018. The copyright holder for this preprint (which was not certified by peer review) is the author/funder, who has granted bioRxiv a license to display the preprint in perpetuity. It is made available under aCC-BY-NC-ND 4.0 International license.

887

888 **Supplementary Table S2. Orthologue prediction improvement with Hmel2.5**
889 **annotation**

890

Statistics	Hmel2	**Hmel2.5**
# genes	33137	41779
# genes in orthogroups	24274	29698
# unassigned genes	8863	12081
% genes in orthogroups	73.3	71.1
% unassigned genes	26.7	28.9
# orthogroups	9320	11062
# species-specific orthogroups	15	18
# genes in species-specific orthogroups	56	105
% genes in species-specific orthogroups	0.2	0.3
Mean orthogroup size	2.6	2.7
Median orthogroup size	2.0	2.0
G50 assigned genes	2	2
G50 all genes	2	2
O50 assigned genes	3252	3638
O50 all genes	5468	6658
# of orthogroups with all species present	9305	11044
# of single-copy orthogroups	6846	8095

891

892

bioRxiv preprint doi: https://doi.org/10.1101/380030; this version posted July 31, 2018. The copyright holder for this preprint (which was not certified by peer review) is the author/funder, who has granted bioRxiv a license to display the preprint in perpetuity. It is made available under aCC-BY-NC-ND 4.0 International license.

Supplementary Table S2. Orthologue prediction improvement with Hmel2.5 annotation

Statistics on orthologue prediction between *H. melpomene* v2 annotation and *H. erato* annotation; and on orthologue prediction between *H. melpomene* v2.5 annotation and *H. erato* annotation.

Supplementary Table S3. Mean and median read depth (RD) for resequenced whole-genome *H. melpomene* samples (van Belleghem *et al.*, 2018)

bioRxiv preprint doi: https://doi.org/10.1101/380030; this version posted July 31, 2018. The copyright holder for this preprint (which was not certified by peer review) is the author/funder, who has granted bioRxiv a license to display the preprint in perpetuity. It is made available under aCC-BY-NC-ND 4.0 International license.

Sample	Species	Sex	Location	Mean RD	Median RD
CAM000531	H. m. rosina	Male	9º87'N 7º96'W	30.59	29
CAM000533	H. m. rosina	Male	9º87'N 7º96'W	28.83	21
CAM000546	H. m. rosina	Male	9º87'N 7º96'W	27.47	26
CAM001841	H. m. rosina	Male	9º87'N 7º96'W	28	28
CAM001880	H. m. rosina	Male	9º87'N 7º96'W	22.76	23
CAM002045	H. m. rosina	Male	9º87'N 7º96'W	25.7	26
CAM002059	H. m. rosina	Male	9º87'N 7º96'W	36.77	32
CAM002071	H. m. rosina	Male	9º87'N 7º96'W	26.43	21
CAM002519	H. m. rosina	Male	9º87'N 7º96'W	26.68	22
CAM002552	H. m. rosina	Male	9º87'N 7º96'W	26.83	22

Supplementary Table S3. Mean and median read depth (RD) for resequenced whole-genome *H. melpomene* samples

H. melpomene resequenced samples mapped to Hmel2 genome using BWA-MEM

Supplementary Figures

bioRxiv preprint doi: https://doi.org/10.1101/380030; this version posted July 31, 2018. The copyright holder for this preprint (which was not certified by peer review) is the author/funder, who has granted bioRxiv a license to display the preprint in perpetuity. It is made available under aCC-BY-NC-ND 4.0 International license.

- **Supplementary Figure S1.** Principal component analysis of gene expression profiles for the 10 whole abdomen male and female samples

- **Supplementary Figure S2.** π_n is negatively correlated to expression level

- **Supplementary Figure S3.** Principal component analysis of gene expression profiles of *H. melpomene* females for 13 ovary samples and 12 gut samples at two different time points

- **Supplementary Figure S4.** Principal component analysis of gene expression profiles of *H. melpomene* females for 13 ovary samples and 12 gut samples at two different time points separated by tissue

Supplementary Figure S1. Principal component analysis of gene expression profiles for the 10 whole abdomen male and female samples

bioRxiv preprint doi: https://doi.org/10.1101/380030; this version posted July 31, 2018. The copyright holder for this preprint (which was not certified by peer review) is the author/funder, who has granted bioRxiv a license to display the preprint in perpetuity. It is made available under aCC-BY-NC-ND 4.0 International license.

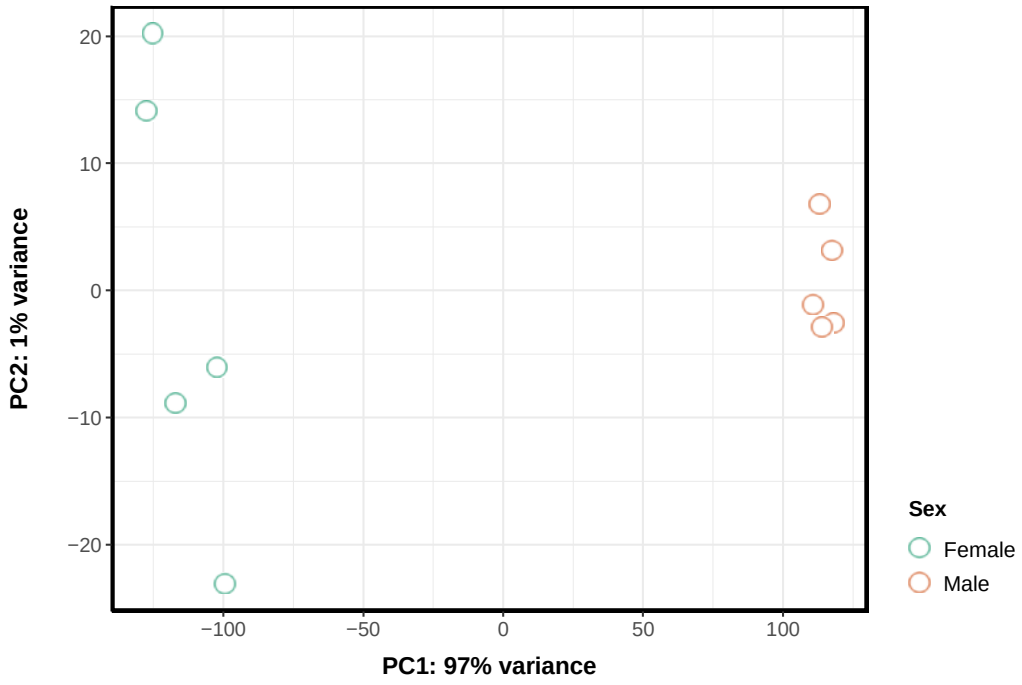

Supplementary Figure S1. Principal component analysis of gene expression profiles for the 10 whole abdomen male and female samples

PCA of the abdomen transformed gene expression count data to the log2 scale (DESeq2, rlog(blind=FALSE)). rlog transformed data minimises

bioRxiv preprint doi: https://doi.org/10.1101/380030; this version posted July 31, 2018. The copyright holder for this preprint (which was not certified by peer review) is the author/funder, who has granted bioRxiv a license to display the preprint in perpetuity. It is made available under aCC-BY-NC-ND 4.0 International license.

differences between samples for rows with small counts and normalizes with respect to library size.

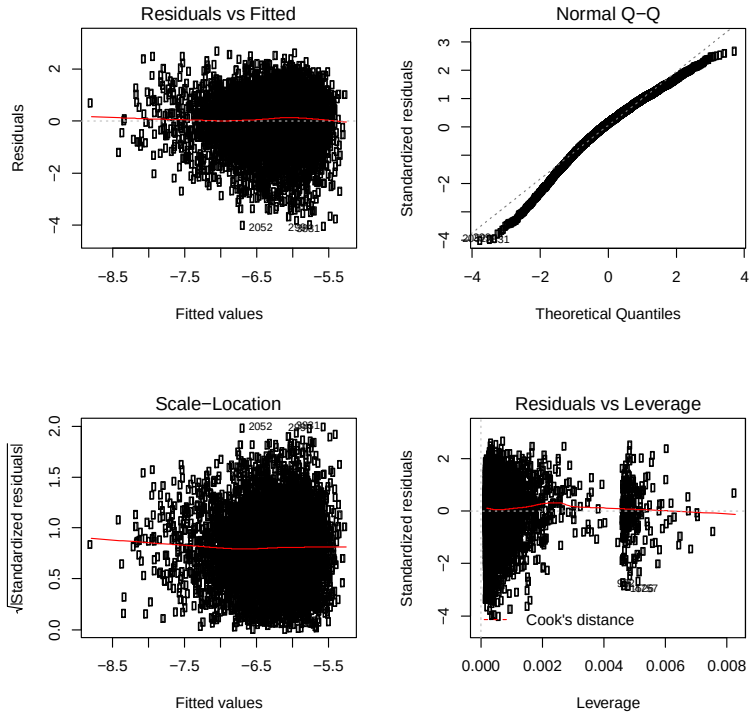

Supplementary Figure S2. π_n is negatively correlated to expression level

A.

bioRxiv preprint doi: https://doi.org/10.1101/380030; this version posted July 31, 2018. The copyright holder for this preprint (which was not certified by peer review) is the author/funder, who has granted bioRxiv a license to display the preprint in perpetuity. It is made available under aCC-BY-NC-ND 4.0 International license.

B.

	estimate	std. Error	value	Pr(>|t|)
(Intercept)	-4.318	0.06	-71.617	< 2e-16
logpiS	0.469	0.015	31.164	< 2e-16
chromosomesex	-0.226	0.071	-3.174	0.002
logRPKMi	-0.035	0.006	-5.529	3.36e-08

Residual standard error: 1.008 on 5428 degrees of freedom
Multiple R-squared: 0.1828, Adjusted R-squared: 0.1824
F-statistic: 404.9 on 3 and 5428 DF, p-value: < 2.2e-16

Supplementary Figure S2. π_n is negatively correlated to expression level

Multiple regression approach shows that π_n was significantly negatively correlated to expression level – autosomal ($P < 0.001$) and Z genes ($P < 0.01$). **A.** Plotted *Residuals vs Fitted* shows spread residuals around the horizontal line

bioRxiv preprint doi: https://doi.org/10.1101/380030; this version posted July 31, 2018. The copyright holder for this preprint (which was not certified by peer review) is the author/funder, who has granted bioRxiv a license to display the preprint in perpetuity. It is made available under aCC-BY-NC-ND 4.0 International license.

without distinct patterns. *Normal Q-Q* follow a straight line with residuals well lined. The *Scale-Location* plot shows residuals spread equally around range of predictors. There is equal variance or homoscedasticity. *Residuals vs Leverage* plot does not identify any influential outliers in the linear regression analysis. **B.** Regression coefficient table. Relationship between π_n and expression.

Supplementary Figure S3. Principal component analysis of gene expression profiles of *H. melpomene* females for 13 ovary samples and 12 gut samples at two different time points

bioRxiv preprint doi: https://doi.org/10.1101/380030; this version posted July 31, 2018. The copyright holder for this preprint (which was not certified by peer review) is the author/funder, who has granted bioRxiv a license to display the preprint in perpetuity. It is made available under aCC-BY-NC-ND 4.0 International license.

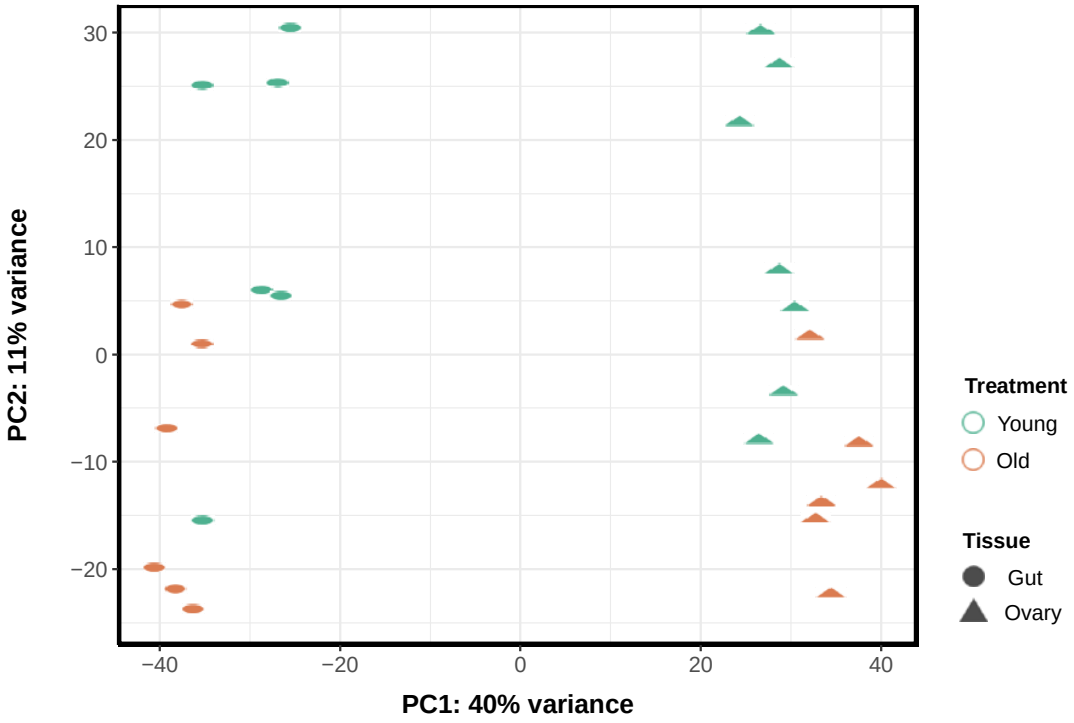

Supplementary Figure S3. Principal component analysis of gene expression profiles of *H. melpomene* females for 13 ovary samples and 12 gut samples at two different time points

PCA of the female ovary and gut transformed gene expression count data to the log2 scale (DESeq2, rlog(blind=FALSE)). rlog transformed data minimises differences between samples for rows with small counts and normalizes with respect to library size.

Supplementary Figure S4. Principal component analysis of gene expression profiles of *H. melpomene* females for 13 ovary samples and 12 gut samples at two different time points separated by tissue

bioRxiv preprint doi: https://doi.org/10.1101/380030; this version posted July 31, 2018. The copyright holder for this preprint (which was not certified by peer review) is the author/funder, who has granted bioRxiv a license to display the preprint in perpetuity. It is made available under aCC-BY-NC-ND 4.0 International license.

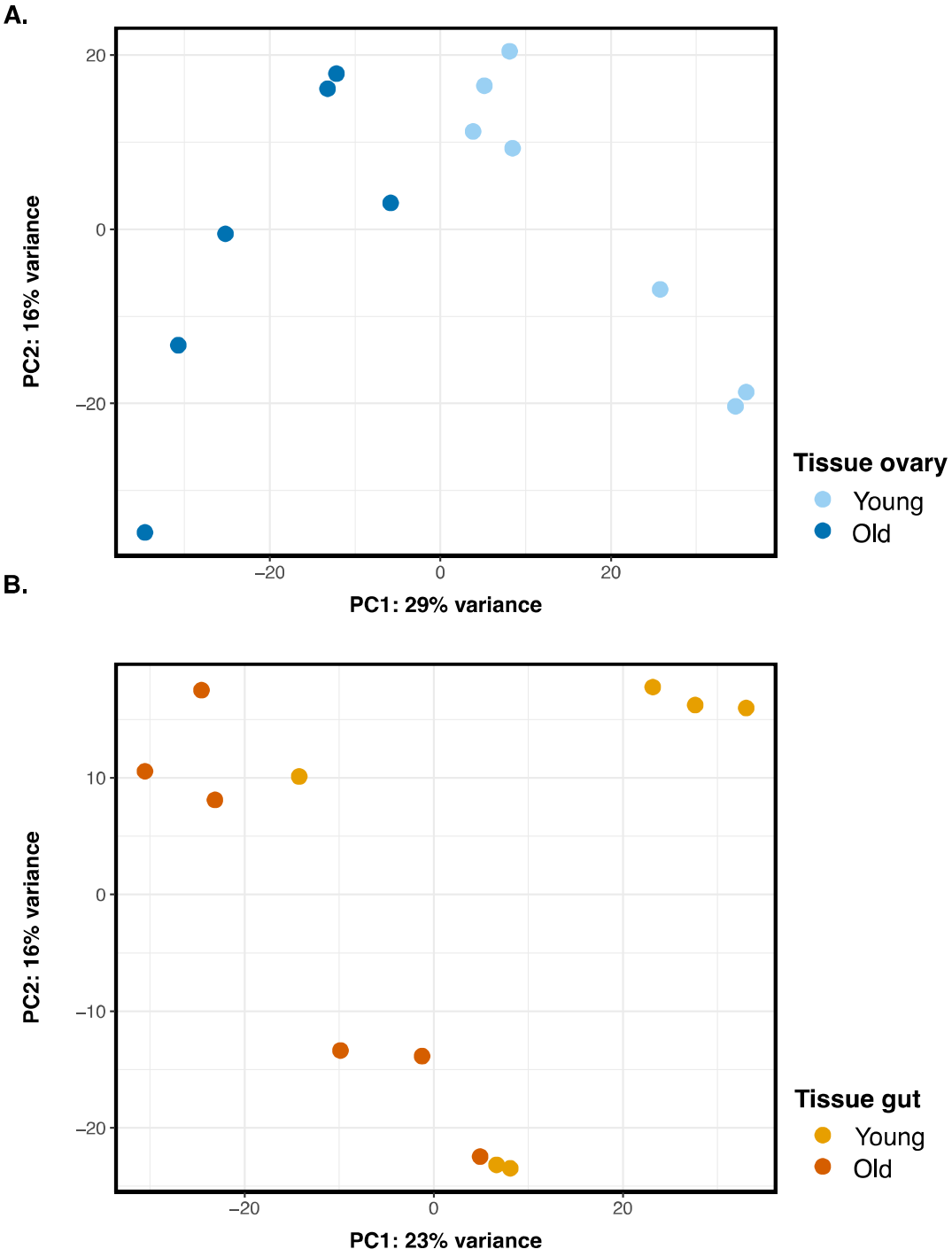

Supplementary Figure S4. Principal component analysis of gene expression profiles of *H. melpomene* females for 13 ovary samples

bioRxiv preprint doi: https://doi.org/10.1101/380030; this version posted July 31, 2018. The copyright holder for this preprint (which was not certified by peer review) is the author/funder, who has granted bioRxiv a license to display the preprint in perpetuity. It is made available under aCC-BY-NC-ND 4.0 International license.

and 12 gut samples at two different time points separated by tissue type

PCA of the female ovary and gut transformed gene expression count data to the log2 scale (DESeq2, rlog(blind=FALSE)) separated by tissue. rlog transformed data minimises differences between samples for rows with small counts and normalizes with respect to library size. **A.** 45% of the variance is explained by PC1 and PC2. PC1 separates young ovary tissue from old ovary tissue and explains 29% of the variance. All the samples cluster by age. **B.** 39% of the total variance is explained by PC1 and PC2. PC1 separates young gut tissue from old gut tissue and explains 23% of the variance. The samples cluster less tightly by age than ovary expression.